OPEN ACCESS

Magneto-transport through single-molecule magnets: Kondo-peaks, zero-bias dips, molecular symmetry and Berry's phase

New Journal of Physics
The open-access journal for physics

Corrigendum

Magneto-transport through single-molecule magnets: Kondo-peaks, zero-bias dips, molecular symmetry and Berry's phase

Maarten R Wegewijs, Christian Romeike, Herbert Schoeller and Walter Hofstetter 2007 *New J. Phys.* **9** 344

New Journal of Physics **13** (2011) 079501
Received 16 November 2010
Published 20 July 2011
Online at http://www.njp.org/
doi:10.1088/1367-2630/13/7/079501

In the paper [1] we reviewed transport through molecular magnets in dependence of magnetic anisotropy and external magnetic fields. Unfortunately, several of the numerical results of this paper are not correct. In particular, in the exchange interaction $J\mathbf{S}\cdot\mathbf{s}$, coupling the SMM to the first site on the Wilson chain in the NRG algorithm, the term JS_zs_z was inadvertently implemented incorrectly. As a result, we did not account for matrix elements of the z-component of the SMM spin operator $\langle i|S_z|j\rangle$ with $i \neq j$, while accounting for those with $i = j$. Here $|i\rangle, |j\rangle$ denote eigenstates of the SMM part of our Hamiltonian $\mathcal{H}_{\rm SMM} = -DS_z^2 + \frac{1}{2}\sum_{n=1,2} B_{2n}(S_+^{2n} + S_-^{2n}) + H_x \cdot S_x + H_z \cdot S_z$ with $D > B_2, B_4$. Thus, the NRG algorithm was applied correctly but using incorrect matrix elements, thereby not capturing the transitions into SMM excited states. This leads to incorrect results only when two conditions are met: (i) the excited states of the SMM are relevant, i.e. J is large enough compared to the largest anisotropy splitting $\Delta = (2S-1)D$, and additionally, (ii) there is transverse anisotropy (B_2, B_4) or a transverse magnetic field. Both conditions (i) and (ii) have to apply at the same time for quantitative errors to occur. Importantly, in the weak exchange limit, i.e. where J is sufficiently weak compared to Δ, condition (i) does not apply: all the results in section 3.1 of [1] are therefore correct. This we checked by explicit recalculation of the results with the corrected code [2]. However, the result in section 3.2 of [1] for large J requires correction. For this we refer to the erratum [2] to [3]. For a very large magnetic field $H_z \gg D, B_2$ the anisotropy becomes unimportant and the eigenstates approach spin eigenstates. Also in this limit, the paper [1] reports the correct suppression and splitting of the Kondo peak. For the above reasons the problem could not be detected in the numerous checks we performed against known results for the Kondo effect for various spins S in a magnetic field but without magnetic anisotropy.

Recalculation of the results of sections 4 and 5 of [1] confirms one of the central conclusions, namely, that the excited states can indeed be involved in the Kondo effect. However, the correct order of magnitude of $T_{\rm K}$ is much smaller, see [2], and the re-entrant behavior of the

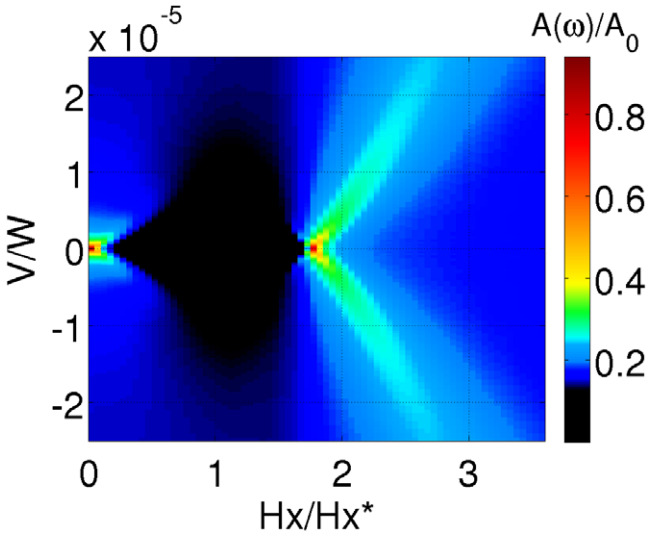

Figure 1. Plot of the spectral function A (normalization $A_0 = \pi^2/4$) as a function of the frequency ω, set equal to the bias voltage V, and the magnetic field energy H_x in units of the diabolical scale $H_x^* = \sqrt{2B_2(D+B_2)}$ for half-integer spin $S = 3/2$ and $D = 10^{-4}$ W and $B_2/D = 0.1$. The value of $J = 0.15$ W is chosen somewhat smaller than the original $J = 0.2$ to reduce the renormalization effect of the positions of the diabolical points.

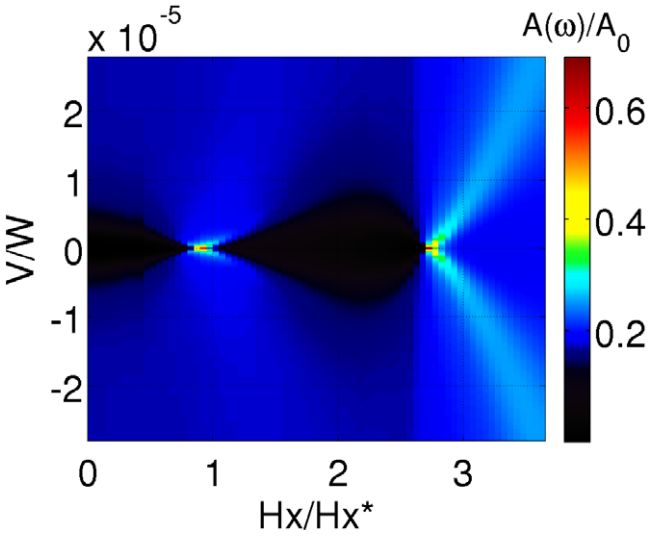

Figure 2. The same as figure 1 except for spin $S = 2$ and anisotropy $D = 2 \times 10^{-4}$ W.

Kondo effect as a function of a longitudinal magnetic field of figures 4, 5 and 7 of [1] is not present. Recalculation of the results of section 5 of [1] confirms the Berry-phase oscillations in the conductance as a function of the external transverse magnetic field H_x (in units of $g\mu_B = 1$). However, at the crossing points of these oscillations, a re-entrant Kondo effect is found, contrary to our statement at the end of section 5.1 of [1]. This instead agrees with the predictions by

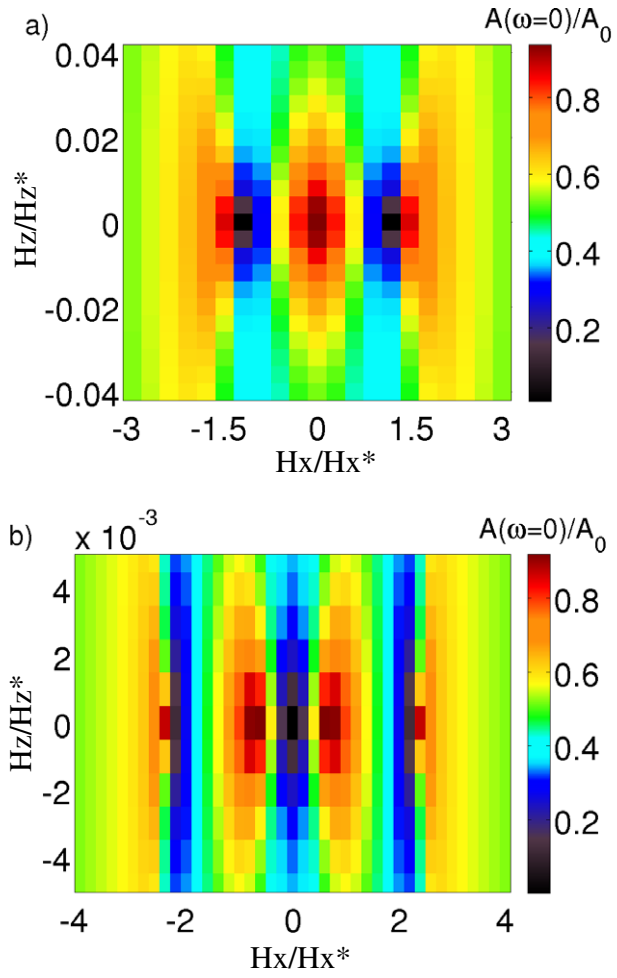

Figure 3. Maps of the spectral function A (normalization $A_0 = \pi^2/4$) evaluated at zero frequency as a function of the longitudinal (H_z) and transverse magnetic fields (H_x) in units of the diabolical scales $H_x^* = \sqrt{2B_2(D+B_2)}$ and $H_z^* = \sqrt{D^2 - B_2^2}$. (a) Spin $S = 3/2$ anisotropy $D = 10^{-4}$ W and other parameters as in figure 1. (b) Spin $S = 2$ and anisotropy $D = 2 \times 10^{-4}$ W and other parameters as in (a).

Leuenberger and Mucciolo [4] in the high-temperature limit that were obtained by a poor-man scaling analysis. In figures 1 and 2, we exemplify the corrected results by showing the dependence of the spectral function on the transverse field for half-integer spin $S = 3/2$ and integer spin $S = 2$, respectively. For the (half-)integer S, the Kondo effect occurs close to odd (even) multiples of the Berry-phase scale $H_x^* = \sqrt{2B_2(D+B_2)}$ up to $2S - 1$, the positions being renormalized due to the large value of J. Similar corrections apply to the zero-bias conductance maps as a function of the longitudinal and transverse fields shown in figure 7 of [1]. In figure 3, we show a representation of the corrected maps demonstrating that the Berry-phase oscillations are suppressed with increasing longitudinal field.

Finally, we mention that the results of [5] are affected only quantitatively [6]. For clarity, we point out that the results of the authors on transport through SMMs other than those mentioned here are not affected in any way by the issue reported here.

Acknowledgment

All of the new calculations above were performed by F May when working at the Institut Für Theoretische Physik, Johann Wolfgang Goethe-Universität, 60438 Frankfurt/Main, Germany. By all means he should be considered to be the first author of the corrigendum, which is however not possible within the policies of *New Journal of Physics*.

References

[1] Wegewijs M R, Romeike C, Schoeller H and Hofstetter W 2007 *New J. Phys.* **9** 344
[2] Romeike C, Wegewijs M R, Hofstetter W and Schoeller H 2011 *Phys. Rev. Lett.* **106** 019902 (E)
[3] Romeike C, Wegewijs M R, Hofstetter W and Schoeller H 2006 *Phys. Rev. Lett.* **97** 206601
[4] Leuenberger M N and Mucciolo E R 2006 *Phys. Rev. Lett.* **97** 126601
[5] Roosen D, Wegewijs M R and Hofstetter W 2008 *Phys. Rev. Lett.* **100** 087201
[6] Roosen D, Wegewijs M R and Hofstetter W 2010 *Phys. Rev. Lett.* **105** 259901 (E)

New Journal of Physics
The open-access journal for physics

Magneto-transport through single-molecule magnets: Kondo-peaks, zero-bias dips, molecular symmetry and Berry's phase

Maarten R Wegewijs[1,2,4], **Christian Romeike**[1], **Herbert Schoeller**[1] **and Walter Hofstetter**[3]

[1] Institut für Theoretische Physik—Lehrstuhl A, RWTH Aachen, 52056 Aachen, Germany
[2] Institut für Festkörper-Forschung—Theorie 3, Forschungszentrum Jülich, 52425 Jülich, Germany
[3] Institut für Theoretische Physik, J W Goethe-Universität Frankfurt, 60438 Frankfurt am Main, Germany
E-mail: m.r.wegewijs@fz-juelich.de

New Journal of Physics **9** (2007) 344
Received 27 April 2007
Published 28 September 2007
Online at http://www.njp.org/
doi:10.1088/1367-2630/9/9/344

Abstract. We theoretically analyse coherent electron transport through a single-molecule magnet (SMM) in the regime where charge fluctuations are suppressed. Using the numerical renormalization group (NRG) technique, we calculate the low-temperature conductance as a function of the SMMs magnetic anisotropy parameters and the strength and orientation of an external magnetic field. We show how the microscopic magnetic symmetry of the molecule affects the transport via a Kondo effect with non-trivial dependence on a longitudinal field. In addition, we show how Berry's phase and the Kondo effect, both associated with reversal of the SMMs spin, appear when both the magnetic field amplitude and direction are varied. It is shown that both effects involve the magnetic excitations of the SMM in an essential way.

[4] Author to whom any correspondence should be addressed.

PII: S1367-2630(07)49605-7

Contents

1. Introduction

Spintronics typically involves transport of electrons where the relativistic coupling of the spin and orbit is particularly important in certain parts of the system. The ultimate limit of such a set-up consists of a single-molecule magnet (SMM) coupled to a source, drain and gate electrode as depicted in figure 1(a). A recent advance in nano-fabrication has been the experimental realization of such a SMM transistor and the investigation of the effects of molecular magnetism on the transport [2, 3]. In such a small molecular device the energy and charge quantization effects are very strong with energy separations on the scale of 50 meV and beyond. As a result a large contribution to the transport through a molecular junction comes from sequential tunnelling of single electrons: typically 'Coulomb diamonds' are observed in the differential conductance [2]–[14], which are a well known sign of quantum-dot behaviour [15]. Interestingly, the measured size- and charge-quantization energies can be substantially smaller than the known bulk values due to the presence of metallic electrodes [6, 16]. Another peculiarity of a molecular junction is that the tunnel coupling typically is so strong that corrections due to cotunnelling (involving coherent electron-hole pairs) [17, 18] and even the Kondo effect [19, 20] are large even at a temperature of a few Kelvin. The spintronic operation of devices exhibiting such standard quantum-dot behaviour by *external* magnetic means (magnetic fields and spin-polarized currents) has been addressed both theoretically in the sequential tunnelling [21]–[25], cotunnelling [26] and the Kondo regime [27, 28], as well as experimentally [10]. In a *magnetic* molecule the intra-molecular exchange and spin–orbit effects give rise to a high-spin ground-multiplet with significant anisotropy splittings, even at zero magnetic field. SMM transistors are distinguished from quantum dots by these peculiar low energy excitations which lie typically on the 1 meV scale, far below the orbital and exchange-level separations. In this contribution, we demonstrate how these *internal* magnetic properties affect the electronic current, *even when connected to normal electrodes at zero magnetic field* in the Coulomb blockade regime where spin-fluctuations dominate the transport. Furthermore, we show that an external magnetic field reveals a rich magneto-transport spectrum from which the magnetic properties of the SMM transistor may be accurately determined *in situ*. Such transport fingerprints are unique to SMMs: they cannot

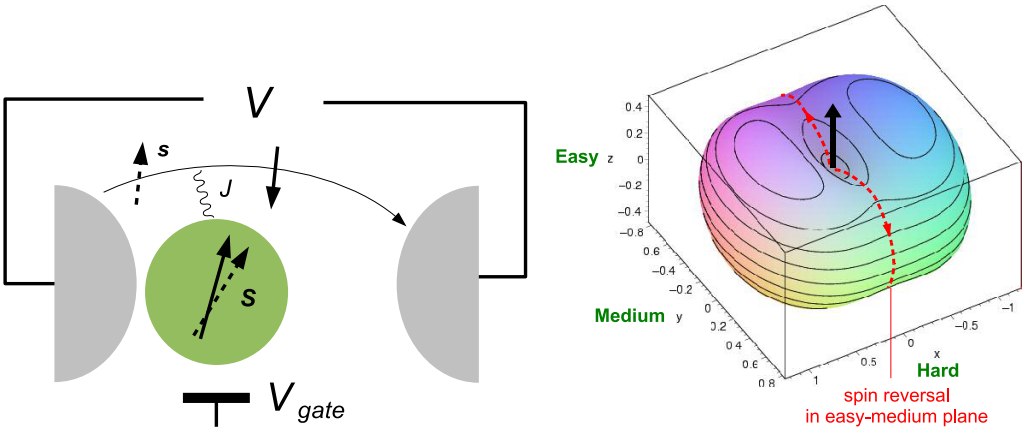

(a) (b)

Figure 1. (a) Transport set-up: a SMM coupled to physical electrodes. The antiferromagnetic exchange $J \sim \Gamma/(\Delta E\rho)$ in equation (2) is induced by *coherent* spin-dependent electron transfer between the physical electrodes, thereby virtually charging the SMM ($\Gamma =$ tunnel coupling, $\Delta E =$ addition energy, $\rho =$ density of states). The conductance essentially measures the equilibrium local density of states or spectral function $\sum_\sigma A_\sigma$ which we calculate using the numerical renormalization group (NRG). (b) Polar plot of the energy of a SMM described by equation (1), with $B_2 = 0.1D$ and $B_4 = H_x = H_z = 0$ and spin of length 1. The dominant uni-axial anisotropy (D) favours the spin (black arrow) to align with the easy z-axis, but maintains a continuous rotation symmetry with respect to this axis. The transverse anisotropy perturbation ($B_2 < D$) breaks this symmetry leaving only the rotation by π as a symmetry element. As a result, in the quantum case the transverse and uni-axial terms are non-commuting operators and the spin can tunnel between eigenstates of S_z. Classically there are two equivalent paths for spin reversal passing through the medium y-axis (dashed red curves). In the quantum case this gives rise to interference involving a Berry phase. A magnetic field modulates the acquired phase difference between the spin-reversal paths for tunnelling [1].

be observed in quantum-dot systems consisting of a small metallic nanoparticles or a carbon-nanotube. They derive from the high spin and discrete molecular symmetry of a SMM and may provide additional evidence in experiments that transport occurs through the targeted molecule.

The hallmark property of a SMM is the quantum dynamics of the large total spin $S > 1/2$ or magnetization. Due to the atomistic details controlled by advanced chemical synthesis a SMM has an *intrinsic* uni-axial anisotropy which designates a preferred axis for the spin, relating to the classical notion of magnet, see figure 1(b). Upon quantization of the spin, the ground-state multiplet exhibits a zero-field splitting (ZFS) due to the anisotropy, which has been studied in great detail with magnetic measurements [29]. From the viewpoint of molecular magnetism, the new aspect of the transport measurements reported in [2, 3] is that ground-state multiplets of several charge states of the SMM are addressed, each split by magnetic anisotropy. In addition, there is a non-commuting transverse anisotropy term that generates coherent tunnelling of the spin through the uni-axial anisotropy barrier which separates states with opposite magnetization.

This is known as quantum tunnelling of the magnetization (QTM) and gives rise to coherent superpositions of spin eigenstates, both as ground and excited states of the SMM, which are split in energy. As a result, the orientation of the spin along the easy-axis of the SMM is completely uncertain, a striking aspect of molecular magnetism. Typically the spin-tunnel splittings are very small in the lower part of the energy spectrum (far below the barrier) and one might expect that this would be difficult to observe in transport. However, it has been shown that the modification of the spin-wave functions due to this spin-tunnelling gives rise to notable effects in the transport in the regime of sequential tunnelling [30, 31], cotunnelling [32]–[34] and especially in the Kondo regime [35, 36]. Suitable SMMs for the observation of such effects of quantum magnetism on the transport have a moderate spin $1 \lesssim S \lesssim 10$ and both a sizable uni-axial and transverse anisotropy.

Application of SMMs as magnetic transistors of molecular dimensions has already been the subject of several proposals in the field of spintronics [31, 33, 34, 37, 38] and quantum-computing [39]. However, before any progress can be made, a crucial step is the understanding of the relation between the microscopic details of a SMM transistor and macroscopic transport quantities. How does one extract the magnetic properties of an individual SMM embedded in an electric circuit from magneto-transport measurements? These include the strength of the magnetic anisotropy barrier, the transverse spin-tunnelling amplitude, the orientation of the SMM's anisotropy tensor with respect to the junction electrodes, as well as the *magnetic symmetry* related to the molecular spatial symmetry. Stabilizing SMMs and accessing their magnetic properties on a surface is difficult [40]–[43], more so for SMMs in a narrow nano-junction. It is not obvious that the SMM retains the precise well-known properties it has in a crystal [44, 45], although synthetic progress has been made in assuring this [2]. Therefore on the level of theoretical description, the essential questions include the following: (i) how does the transport reflect the above magnetic properties if charge fluctuations are dominant? How is it affected by a significant dependence of the magnetic properties of the SMM on the charge state? Such a dependence is well known from electro-chemical studies of SMMs. We recently addressed this question and found that the quantized magnetic states can be resolved in zero-field single-electron transport [2, 30], which was found experimentally [2, 3]. See [39] for the corresponding transport phenomena for single-molecule antiferromagnets. (ii) At low temperature and bias voltage, in appropriate gate voltage regimes the molecular charge is stabilized by charge- and energy-quantization. Then, in addition to the intrinsic spin-tunnelling, the molecular spin can fluctuate due to exchange scattering of the electrons. This results from electron tunnelling processes where the molecule is only virtually charged. Do these spin-dependent processes cooperate or compete in the spin reversal and how do they effect the transport? Is there a *Kondo effect* associated with exchange scattering and how is it modified? In the presence of anisotropy, the reversal of a spin $S > 1/2$ by tunnelling involves interference effects related to a geometric or *Berry phase*, as explained in figure 1(b). What is the joint impact of the Kondo effect and the spin Berry phase on the transport, which both relate to spin reversal? In this paper, we will address these questions relating to the spin-fluctuation regime using the most basic transport model presented in the following section.

2. Minimal transport model for SMMs

SMMs are typically organo-metallic complexes made up from metal ions with nonzero spin ground states held together by bridging ligands which mediate exchange interactions. These ions exhibit a ground-state splitting at zero magnetic field: since the local environment of such an

ion is not spherically symmetric (ligand/crystal field effect) the spin–orbit coupling effectively gives rise to an anisotropic potential for the spin, see figure 1(b). We disregard here complications arising from nonzero angular momentum of the ions, which plays a role in some SMMs. The total molecular spin of the coupled ions 'inherits' this anisotropy from its constituents, as can be shown by tensor operator techniques [46]. The non-trivial dynamics of the total spin due to the anisotropy is governed by an effective spin Hamiltonian [46] given by

$$H_{\mathrm{SMM}} = -DS_z^2 + \tfrac{1}{2}\left[B_2\left(S_+^2 + S_-^2\right) + B_4\left(S_+^4 + S_-^4\right)\right] + \sum_{i=x,z} H_i S_i, \tag{1}$$

where S_i is the projection of the SMM's spin on the i-axis where $i = x, y, z$ and $S_\pm = S_x \pm iS_y$ are the ladder operators. The terms in equation (1) describe, respectively, the easy-axis magnetic anisotropy of the molecule, the transverse anisotropy perturbations and the coupling to a magnetic field along the easy axis (H_z) and transverse to it (H_x). The g-factors are absorbed into the magnetic field components. The transverse anisotropy terms generate the quantum tunnelling of the magnetic moment, since they do not commute with the easy-axis term. One can say that the spin-tunnelling is generated by the *molecular* symmetry: since the magnetic ions take up discrete positions within the molecule, in equation (1) terms are allowed which exhibit no continuous rotational symmetry; see also the caption of figure 1(b). Controlling these terms by chemical synthesis has been the subject of the field of molecular magnetism, see for a review [29]. The atomistic details of the molecule thus determine the discrete symmetry of the dominant transverse terms, and two limiting cases are of interest here: (i) low symmetry transverse term: $B_2 > 0$ and $B_4 = 0$. Since $(S_+^2 + S_-^2)/2 = S_x^2 - S_y^2$, the x-axis is the magnetic hard-axis of the molecule, see figure 1(b). (ii) High symmetry transverse term $B_4 > 0$ and $B_2 = 0$. The B_2 (B_4) term has a 2-fold (4-fold) rotation-symmetry axis and the Hilbert space is split into 2 (4) subspaces for $H_x = 0$ for any longitudinal magnetic field (which preserves the rotational symmetry about the z-axis). In contrast, a finite transverse magnetic field H_x reduces the symmetry and couples all these subspaces. A central point of the paper is that the existence of uncoupled subspaces of different symmetry gives rise to a strong dependence of the magnetic wavefunctions on the anisotropy parameters and external magnetic fields which can be detected by a transport current.

In the regime where the applied voltages, charging effects and low temperature suppress single-electron tunnelling [35], we can consider the ground multiplet of a single charge state of the SMM described by a well defined value of the spin S. In the absence of charge fluctuations, the tunnel coupling to two physical electrodes results in exchange scattering H_{ex} of electrons from a effective electrode H_{res}. The Hamiltonian of the complete system then reads: $H = H_{\mathrm{SMM}} + H_{\mathrm{ex}} + H_{\mathrm{res}}$ where

$$H_{\mathrm{ex}} = J\boldsymbol{S}\cdot\boldsymbol{s}, \tag{2}$$

$$H_{\mathrm{res}} = \sum_{k\sigma} \epsilon_{k\sigma} a_{k\sigma}^\dagger a_{k\sigma}. \tag{3}$$

Equation (2) describes the exchange coupling of the molecular spin to the effective reservoir equation (3) (bandwidth $2W$ and constant density of states ρ). The electronic states are labelled by $k\sigma$ and denote the even combination of left and right physical electrode states [19, 20]. The local electron spin in the reservoir is $\boldsymbol{s} = \sum_{kk'}\sum_{\sigma\sigma'} a_{k\sigma}^\dagger \boldsymbol{\tau}_{\sigma\sigma'} a_{k'\sigma'}/2$ where $\boldsymbol{\tau}$ is the Pauli-matrix vector. The exchange coupling J is induced by virtual electron tunnelling processes

and is antiferromagnetic due to the strong energy- and charge-quantization effects [47], see caption of figure 1. We have calculated the low temperature conductance $G(V) = \mathrm{d}I(V)/\mathrm{d}V = (e^2/2)\sum_\sigma A_\sigma(V)$ through the SMM from the spectral function $A_\sigma(\omega)$ obtained using Wilson's NRG [48, 49] within the T-matrix approach [50], accounting for all eigenstates of H_{SMM}, see [35, 36]. The magnetic structure of the SMM enters the calculation through matrix elements of the spin operator S between the exact eigenstates of the molecular Hamiltonian, equation (1), see next section. This approach is non-perturbative in J and describes correctly the enhancement of the zero-bias conductance due to the Kondo effect. For a SMM coupled asymmetrically to the electrodes, see figure 1(a), for which deviations of the magnetic state occupations from equilibrium are small, $G(V)$ as calculated above, also gives the conductance a small, finite bias. We will restrict our attention to this situation, since we can then distinguish whether there is a peak or dip in the conductance, and we can identify the splitting of the Kondo peak by a magnetic field as such from the NRG results. Below we will always discuss the experimentally measurable conductance G as a function of the experimentally controllable variables (voltage and magnetic field).

The remaining part of the paper is organized as follows. In section 3, we explain why the zero-field transport depends sensitively on the magnetic parameters of the SMM. Due to the cooperation of intrinsic spin-tunnelling and exchange scattering processes related to the transport a non-trivial Kondo effect can occur in SMMs. The strength of the Kondo zero-bias conductance *peak* depends non-monotonically on the transverse anisotropy due to the occurrence of anti-crossings of the excitations of the SMM induced by the spin-tunnelling. In section 4, we demonstrate that this Kondo effect also shows re-entrant dependence on a magnetic field applied along the easy axis due to similar avoided crossings. We show that this effect reveals the *symmetry* of the dominant transverse anisotropy term, allowing it to be extracted from a measurement. In section 5, we demonstrate that the *Berry phase* associated with reversal of the spin can be detected in transport measurements by scanning the magnetic field vector in the plane of the SMMs easy and hard axis. In particular, we show that this phase directly modulates a pronounced zero-bias *dip* in the conductance.

3. Zero magnetic field: Kondo effect and spin-tunnelling

In the present and following sections the transport involving exchange scattering is discussed. Since the ground state spin-multiplet of the SMM is split, one has to distinguish two regimes, in contrast to the standard $S = 1/2$ Kondo problem: weak exchange $\Delta \lesssim J$ and strong exchange, $\Delta \ll J$, where Δ denotes the energy separation of the lowest two states from the rest of the spectrum. For $B_2, B_4 S^2 \ll D$ this ZFS is denominated by the uni-axial anisotropy barrier: $\Delta \approx (2S-1)D$. The weak exchange regime allows for a simpler physical picture since the SMM ground doublet is responsible for the transport properties. On the other hand it might be experimentally less favourable since the Kondo effect is weak i.e. typically low temperatures are required. In the strong exchange regime all magnetic excitations of the SMM participate in transport basically because the Kondo energy scale $T_{\mathrm{K}}(J, \Delta)$ associated with the excitations can reach the energy splitting Δ for sufficiently large $J \gg \Delta$. This leads to a series of effects that are related to the unique magnetic properties of these molecules. Along a similar vein, we recently demonstrated a Kondo effect involving resonant exchange scattering of an excited triplet state in the presence of a discrete vibrational mode [51]. Typically one experimentally finds strong

tunnelling [6, 8, 12], [52]–[54], giving rise to a standard $S = 1/2$ Kondo effect with Kondo temperatures in excess of 200 K∼20 meV [54]. Therefore depending on the SMM parameters (mainly D and S) and the junction parameter J either regime may be accessible in experiments.

3.1. Weak exchange scattering

The Kondo effect is a many-body phenomenon involving scattering processes in all orders of $H_{\rm ex}$ [55]. It results in a screening of internal degrees of freedom of the scattering centre and is evidenced by a resonance peak in the conductance at low bias [20, 21]. For a SMM the characteristic energy scale, the Kondo temperature $T_{\rm K}$, depends non-trivially on the spin S and the magnetic parameters B_2, B_4, D. We have calculated this dependence rigorously using the NRG [35]. A more intuitive picture of the processes leading to Kondo correlations in a SMM is obtained by truncating the spectrum, keeping only the two degenerate ground eigenstates $|\pm\rangle$ of $H_{\rm SMM}$. One obtains an effective spin-1/2 Kondo model $H_{\rm eff} + H_{\rm res}$ with

$$H_{\rm eff} = \sum_{\alpha=x,y,z} j_\alpha P_\alpha s_\alpha, \tag{4}$$

where the pseudo-spin operators are defined through $P_x, iP_y = (|+\rangle\langle -| \pm |-\rangle\langle +|)/2$ and $P_z = (|+\rangle\langle +| - |-\rangle\langle -|)/2$. The effective exchange constants depend on B_2, B_4, D and S through the matrix elements of the spin operator:

$$j_z = 2J\langle +|S_z|+\rangle > 0, \tag{5}$$

$$j_{x,y} = J\langle +|S_+ \pm S_-|-\rangle. \tag{6}$$

Importantly, these constants are *completely* anisotropic, except for special values of the parameters where they are axially anisotropic (see below). A central result is that for weak transverse anisotropy of the form $B_{2m}(S_+^{2m} + S_-^{2m})/2$ the Kondo effect can occur only if the spin is commensurate with the magnetic symmetry in the following sense:

$$\frac{2S-1}{2m} = \text{integer}. \tag{7}$$

Thus at zero-magnetic field the Kondo effect can only occur for half-integer spin SMMs. If the transverse anisotropy has a symmetry higher than that of B_2, additional half-integer spin values not satisfying (7) are excluded. This 'spin-selection rule' (7) can be checked very easily provided the spin and the symmetry of the dominant transverse term of the molecular magnet are known.

Before deriving this 'spin-selection rule', we show that it expresses a simple commensurability problem for weak transverse anisotropy $B_{2m}S^{2(m-1)} \ll D$. This is illustrated in figure 2. We choose the $|+\rangle$ state such that $j_z > 0$ without loss of generality and we want to see if the exchange interaction can reverse the pseudo-spin from $-$ to $+$. This amounts to finding processes which can reverse the SMM spin from $M = -S$ to $M = +S$ using *only* the spin raising operator S_+ (see below). Firstly, an exchange scattering process increases M to $-S + 1$, while flipping the spin of transferred electron down. Clearly the usual underscreened Kondo resonance for $S > 1/2$ is suppressed by the energy penalty for this process $\Delta \approx (2S-1)D$ introduced by the uni-axial anisotropy. Subsequently, due to the discrete molecular symmetry the transverse

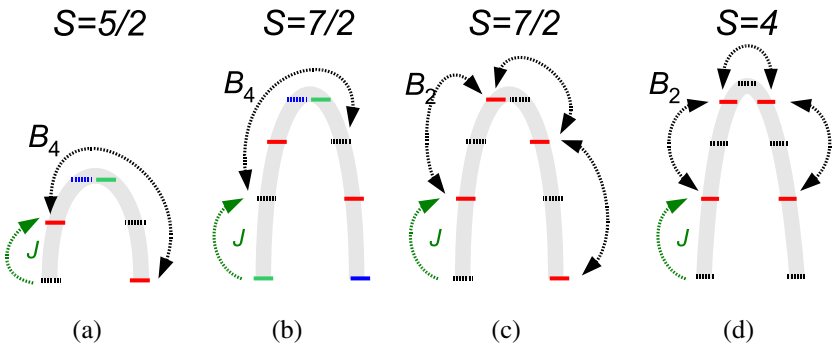

Figure 2. 'Spin-selection rule': the Kondo effect can occur only if the spin is commensurate with the magnetic symmetry. The levels depict spin states M where $M = -S$ on the lower left side of the parabola and increases linearly to $M = S$ on the lower right side. Subsets of states which are not coupled by the transverse anisotropy term have different line style (full, dashed) and colour.

term allows the spin to tunnel by virtually crossing the uni-axial anisotropy barrier in *big, even* steps $M' - M = 2m$. Odd steps are forbidden by time-reversal symmetry. For a commensurate odd spin value S one can reach $M = S$, figure 2(a), whereas for incommensurate odd value one ends up in an excited state, breaking the resonance condition for the Kondo effect, figure 2(b). In a similar way, it is evident that for any half-integer spin and low symmetry anisotropy the exchange scattering can reverse the spin and the Kondo effect occurs, figure 2(c). Finally, along the same line, one finds that an integer spin value S is incommensurate with transverse anisotropy of *any* symmetry, as it always breaks the Kondo resonance condition, figure 2(d).

The low energy properties of the above pseudo-spin scattering model can be understood analytically from a poor-man scaling analysis [56]. In this approach, one scales the conduction-bandwidth W down and simultaneously adjusts the coupling constants through second order perturbation theory to keep the physics described by the model invariant [57]. This adjustment is described by the scaling equations:

$$\frac{\mathrm{d}\, j_\alpha}{\mathrm{d}\ln W} = -\rho j_\beta j_\gamma, \tag{8}$$

where α, β, γ are cyclic permutations of x, y, z [58] and the initial values are given by equations (5) and (6). This effectively amounts to a non-perturbative treatment of the exchange scattering. This approach breaks down when one coupling constant diverges at a scale $W = T_\mathrm{K}$: this allows one to extract the Kondo temperature. In order to solve (8) we use the fact that specification of any two scaling invariants $j_\alpha^2 - j_\beta^2, \alpha \neq \beta$ defines a three-dimensional scaling curve. Inversion of any pair of j_α, j_β leaves the scaling equations invariant, whereas inverting a single one reverses the flow. Interestingly, all scaling trajectories flow to the strong coupling limit except those in planes of uni-axial symmetry, $|j_\alpha| = |j_\beta| < |j_\gamma|$ with $j_\alpha j_\beta j_\gamma < 0$. In the latter case one has a ferromagnetic fixed line which is unstable with respect to infinitesimal perturbations perpendicular to it which are typically present in our model. If the effective exchange constants lie close to this line the Kondo temperature will thus be strongly suppressed. The scaling equations

can be integrated and for $|j_z| \geqslant |j_x| \geqslant |j_y|$ with $|j_z| \neq |j_y|$, we find for the Kondo temperature

$$\ln(T_K/W_{\rm eff}) = -\frac{1}{\rho\sqrt{{j_z}^2 - {j_y}^2}}\mathrm{cs}^{-1}\left(\frac{|j_y|}{\sqrt{{j_z}^2 - {j_y}^2}}\left|\frac{{j_z}^2 - {j_x}^2}{{j_z}^2 - {j_y}^2}\right.\right), \tag{9}$$

here $\mathrm{cs}^{-1}(u|m)$ is the inverse of the elliptic integral $\mathrm{cs}(u|m)$, see [59]. In the uni-axial planes $|j_z| = |j_x|$ or $|j_x| = |j_y|$ equation (9) reduces to the well-known expressions for easy-axis anisotropy [60, 61] since $\mathrm{cs}^{-1}(u|0) = \arctan(1/u)$ and $\mathrm{cs}^{-1}(u|1) = \mathrm{arctanh}(\sqrt{1+u^2})$. In this scaling procedure the upper bound of the Kondo scale T_K is set by the effective bandwidth $W_{\rm eff}$ from which the scaling is started. For this one should take the ZFS Δ, separating the Kramers-degenerate ground state from the other excitations of the SMM. The ZFS Δ depends on the SMMs parameters D, B_{2n}, S and typically is on the order of $(2S-1)D \sim 0.1$ meV i.e. $T_K \lesssim 1$K. If T_K reaches Δ the Kondo effect persists but the scattering becomes more complicated, as discussed in the next section.

The transverse anisotropy terms of the SMM generate the transverse exchange couplings (6) which are essential to the Kondo effect. For the typical case of a small transverse perturbation one has $|j_x|, |j_y| < j_z$. Then, the Kondo effect can develop except when $|j_x| = |j_y|$ and $j_x j_y < 0$, which using equation (6), gives the condition

$$\langle +|S_+|-\rangle \neq 0, \tag{10}$$

i.e. the molecular spin raising operator in the exchange interaction has to flip the pseudo-spin from down $(-)$ to up $(+)$. This leads to the 'spin-selection rule' (7) discussed above. For a dominant low-symmetry transverse term, $B_2 < D$, the criterion (10) is always fulfilled for any half-integer spin. As a function of B_2 the Kondo temperature T_K given by equation (9) shows a single broad maximum at $B_2 = D$, in agreement with the NRG results [35]. Since the spin-tunnelling generated by B_2 assists the exchange scattering in reversing the total spin, T_K increases exponentially as one approaches this peak from $B_2 < D$. In contrast to this, for a high symmetry transverse term $B_4 S^2 \ll D$ condition (10) is violated for spin values $S = (7+4k)/2$, $k = 0, 1, 2, \ldots$: the ground states are linear combinations of spin eigenstates with $M = \mp S \pm 4q$, $q = 0, 1, 2, \ldots$ and can only be connected by the spin lowering operator. The Kondo effect is thus suppressed by the high symmetry of the SMM in the weak exchange regime, see [35].

3.2. Strong exchange scattering

In the strong exchange regime it is no longer possible to discuss the Kondo effect using only the two ground states of the SMM and the behaviour discussed above may break down. To appreciate the complexity of the scattering in this regime it is useful to change to the exact representation of equation (2) in the eigenbasis of $H_{\rm SMM}$ and consider the two cases of low and high symmetry where only B_2 or B_4 is nonzero, respectively. The eigenstates are mixtures of different spin eigenstates $|S, M\rangle$ and are denoted by $|nl\sigma\rangle$. Examples are shown in figure 3. There are disjoint subspaces due to the symmetry of $H_{\rm SMM}$ which come in pairs, one subspace mapping onto the other under the operation of time-reversal ($|S, M\rangle \to (-1)^{S-M}|S, -M\rangle$). The members of each pair are distinguished by $\sigma = \pm$. For high-symmetry anisotropy B_4, there are two such pairs of subspaces requiring an extra label $n = 1, 2$ to distinguish them ($n = 1$ for low-symmetry anisotropy B_2). Finally, within each $n\sigma$ subspace $l = 1, 2, \ldots$ counts the states in

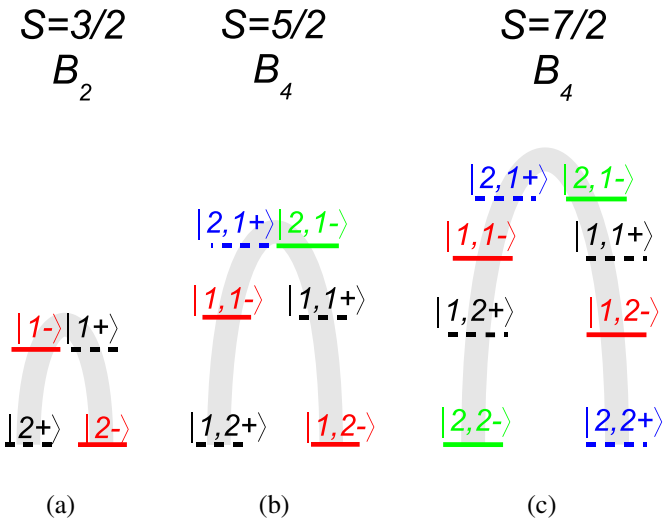

Figure 3. (a)–(c) Schematic eigenspectra of H_{SMM} for weak transverse anisotropy perturbations with low (a) and high (b) and (c) symmetry. The states are labelled as $|n, l\sigma\rangle$ as described in the text (in (a) the only possible value $n = 1$ is not indicated for clarity). States from the same subspace have matching line style (full, dashed) and colour. Note the structural similarity between the spectra in (a) and (b).

order of *decreasing* energy. In this basis equation (2) reads

$$H_{\mathrm{ex}} = \sum_{\substack{nl \\ n'l'}} \left(\sum_{i=x,y} J^{i}_{nl,n'l'} P^{i}_{nl,n'l'} s_i + \sum_{\sigma} J^{z}_{nl,n'l'\sigma} |nl\sigma\rangle\langle n'l'\sigma| \, s_z \right). \tag{11}$$

The first, transverse, term describes the spin-scattering involving a pair of states $|nl+\rangle$ and $|n'l'-\rangle$ in terms of pseudo-spin-1/2 operators $P^{x}_{nl,n'l'}, iP^{y}_{nl,n'l'} = (|nl+\rangle\langle n'l' - | \pm |n'l'-\rangle\langle nl + |)/2$ with effective exchange couplings

$$J^{x,y}_{nl,n'l'} = J\langle nl + |S_+ \pm S_-|n'l'-\rangle. \tag{12}$$

The longitudinal couplings read $J^{z}_{nl,n'l'\sigma} = J\langle nl\sigma|S_z|n'l'\sigma\rangle$. We point out that longitudinal spin operators $P^{z}_{nl,n'l'} = (|nl+\rangle\langle nl + | - |n'l'-\rangle\langle n'l' - |)/2$ can only be introduced in a *unique* way if an approximative projection onto a single pair of states is made. The representation (11) makes explicit that the transverse exchange scattering of an electron, flipping its spin from $\downarrow$ to $\uparrow$, induces a transition on the SMM, $|nl\sigma\rangle \rightarrow |n'l' - \sigma\rangle$. Importantly, there is no selection rule, neither on l, l' nor on n, n' i.e. the transition may involve states of different energy. This means that in a SMM $\propto S^2$ transitions between internal magnetic states are involved in the exchange scattering. In contrast, for a spin S without transverse anisotropy only $2S$ transitions are possible due to selection rules (i.e. continuous rotation symmetry). It is this large amount of possible transitions, combined with the complicated dependence of the corresponding amplitudes in equation (11) on the quantum numbers n, n', l, l' and on the parameters B_2, B_4, D which gives rise to the rich transport characteristics of SMMs. For strong exchange the resonant scattering involving the excited states may have a corresponding energy scale $T_{\mathrm{K}}(J, \Delta)$ on the order of the energy splitting Δ. Then the coupled system of SMM and electrodes can sustain a Kondo effect, even

though the ground state of the isolated SMM may be non-degenerate. This requires the NRG technique for a proper treatment. Only in the weak exchange regime one can reduce equation (11) to the effective pseudo-spin 1/2 model of section 3.1 by neglecting the excitations.

The importance of the excited states is clearly seen already for low symmetry anisotropy: T_K calculated with the NRG *oscillates* as a function of B_2, instead of showing a single maximum at $B_2 \sim D$ as in the weak exchange regime [36]. The dips in T_K arise due to *anticrossings* of SMM eigenstates which are traversed as B_2/D is varied. At such an anticrossing many of the transverse exchange couplings (12) vanish as explained in [36]. Basically, at anticrossings certain magnetic states $|S, M\rangle$ of which the eigenstates are composed interchange their roles and there is a cancellation of the matrix elements of S_+ and S_- in equation (12) [36]. The interesting new aspect of a high symmetry transverse term B_4 ($B_2 = 0$) is that there is no Kondo effect for weak exchange and incommensurate half-integer spin values $S = (7 + 4k)/2$, $k = 0, 1, 2, \ldots$. For small $B_4 \ll D/S^2$ condition (10) is violated for the ground Kramers' doublet. However, the *excited* states do support a Kondo effect which is evidenced by the dramatic dependence of T_K on the strength of the transverse term B_4 in the weak exchange regime noted in [35]. Due to the high symmetry, states from the different subspaces $n = 1, 2$ (cf equation (11)) can intersect in energy as one varies B_4. For example, for $S = 7/2$ the Kondo effect suddenly appears beyond the threshold $B_4 \gtrsim 1.5D/S^2$ due to a change of the SMMs ground state: condition (10) is obeyed for the new ground doublet and T_K jumps to a nonzero value [35]. A similar effect occurs when the exchange scattering becomes strong: the restoration of the Kondo effect suppressed by symmetry and the magnetic field dependence are discussed in the next section.

4. Longitudinal magnetic field: magnetic symmetry

In the weak exchange limit the magnetic field has the sole effect of suppressing the Kondo peak. This can be seen explicitly from the mapping onto the pseudo-spin 1/2 Kondo model (4) for which this behaviour is known. In contrast, in the strong exchange regime which we will consider from here on, the Kondo effect shows a rich re-entrant behaviour as a longitudinal magnetic field H_z is varied [36]. This is due to anticrossings of excited eigenstates of the SMM as discussed above, which are now induced by the external magnetic field. Here we show how this behaviour is strongly modified if a transverse anisotropy term with high symmetry B_4 is important or even dominating the B_2 term. Two striking demonstrations of this are shown in figures 4 and 5, which were calculated using the NRG.

For $S = 5/2$ the high symmetry does not suppress the Kondo effect at zero-field in the weak exchange limit. However, the magnetic field dependence in the strong exchange limit shows a peculiarity. The magneto-conductance for a low-symmetry anisotropy and lower spin $S = 3/2$ shown in figure 4(a), seems closely related to that for $S = 5/2$ and high-symmetry anisotropy, figure 4(b). The result for low-symmetry with the same spin, figure 4(c), is clearly distinct. The reason for the seemingly smaller spin of the SMM from the magneto-conductance is that the Kondo effect is only sensitive to anticrossings of states: the upper two states in figure 3(b) do not anticross with any other state. The strong modulation of the conductance due to an anticrossing near $H_z = 3D$ occurring in figure 4(c), is absent in figure 4(b), where the levels cross due to the high symmetry, see figure 4(e). One can reveal the symmetry by applying a small transverse field which mixes the degenerate states. For sufficiently small H_x this will first have a drastic effect on the Kondo effect near all crossings. This indeed happens before the Kondo effect is

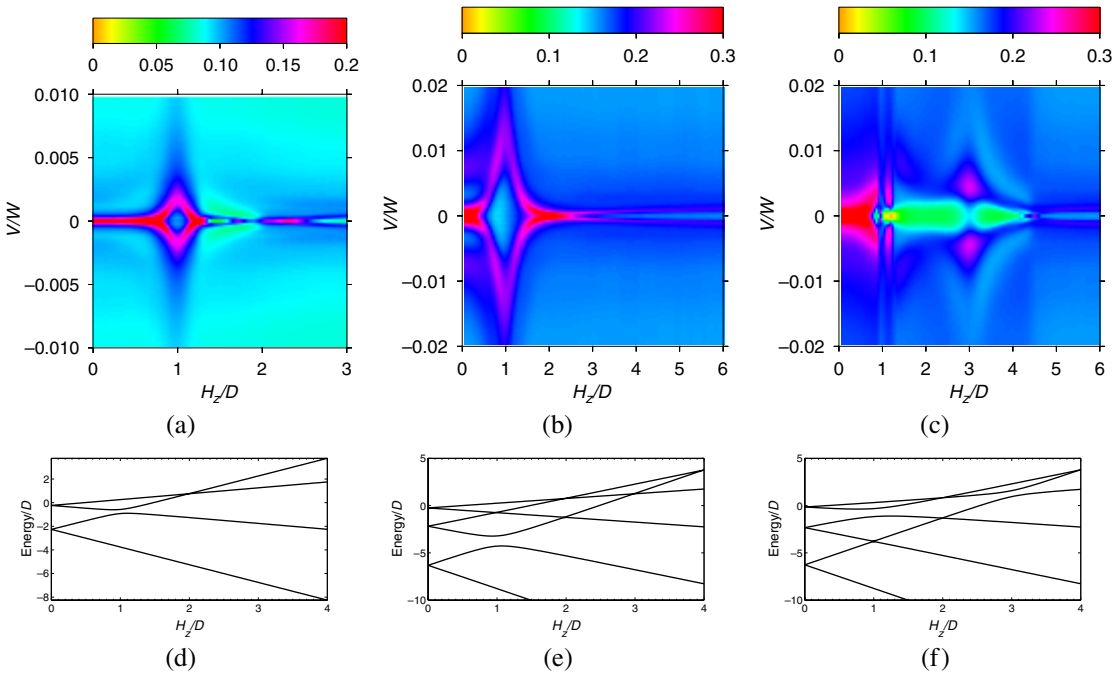

Figure 4. (a)–(c): conductance map as function of the longitudinal field H_z and bias V: (a) $S = 3/2$, and $B_2 = 0.1D$ (b) $S = 5/2$ and $B_4 = 0.02D$ (c) $S = 5/2$ and $B_2 = 0.01D$. (d)–(f): Corresponding spectra of the molecular Hamiltonian as function of the longitudinal field H_z. Other parameters: $J = 0.15W$, $D = 10^{-4}W$.

suppressed altogether at larger values of H_x. In particular, in figure 4(b) a additional modulation of the Kondo effect will appear for finite H_x at $H_z = 2D, 3D, 4D$, whereas in figure 4(a) this will happen only at $H_z = 2D$. This reveals both the true spin value as well as the symmetry of the transverse anisotropy.

An even more striking demonstration is the Kondo effect for $S = 7/2$ around zero-field in figure 5(a): it is *entirely* due to the SMM excited states since the transverse anisotropy is small here, $B_4 < 1.5D/S^2$. In the weak exchange limit at $H_z = 0$ the Kondo effect is completely suppressed in accordance with 'spin-selection rule' (10) due to the high symmetry and the incommensurable value of the spin, cf section 3.1. Here J is so large that a Kondo effect due to the resonant scattering in the excited states is supported. Again the strong modulations of the Kondo effect at $H_z = D, 3D$ are related to the anti-crossings in the spectrum. Finally, figures 5(a)–(d) show the crossover from a pure high symmetry perturbation ($B_4 \neq 0$, $B_2 = 0$), figure 5(a), to a pure low symmetry perturbation ($B_2 \neq 0$, $B_4 = 0$), figure 5(d), as we vary B_2 relative to B_4. Already a weak $B_2 < B_4S^2$ induces an additional anticrossing at $H_z = 5D$ which appears as a sharp dip in the conductance, see figure 5(b). Further increase of $B_2 > B_4S^2$ results in a broadening of this anticrossing and the dip, see figure 5(c). The additional strong modulation of the conductance for $H_z < 5D$ is very similar to that in the case of pure low-symmetry shown in figure 5(d). This crossover may be realized in an experimental set-up by perturbing the molecular geometry by electric fields or nano-mechanical techniques: starting from a SMM with dominant high symmetry, one may detect a low-symmetry deformation in the magneto-transport by the appearance of the new anticrossing at $H_z = 5D$ as the ratio B_2/B_4 is varied. We note that this

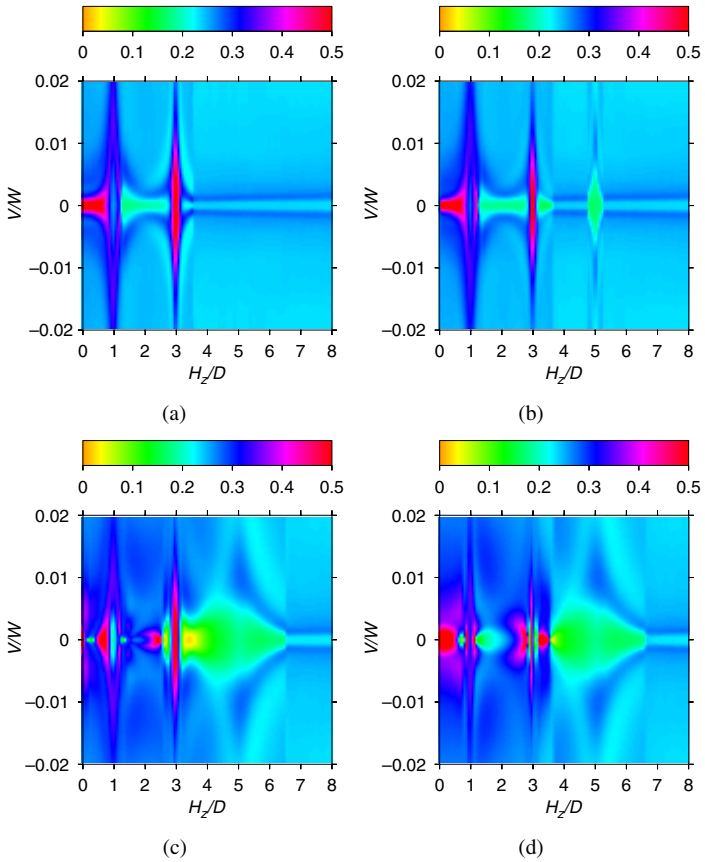

Figure 5. Conductance map as function of the longitudinal field H_z and bias V for $S = 7/2$, $B_4 = 0.002D$ and (a) $B_2 = 0$, (b) $B_2 = 0.01D$, (c) $B_2 = 0.1D$ and (d) for $B_4 = 0$, $B_2 = 0.1D$. Other parameters: $J = 0.15$, $D = 10^{-4}W$.

effect is qualitatively distinct from the effect of a transverse field which would also induce anticrossings at *even* multiples of D.

5. Berry phase effects on the magneto-conductance

We now consider the dependence of the conductance on a magnetic field with transverse components. So-called diabolical fields have been at the focus of intense theoretical research and have been demonstrated experimentally in magnetization measurements [62]. At these field points, eigenstates of the SMM become exactly degenerate due to a quenching of the spin-tunnelling by interference involving a *Berry phase* [1, 63]. In the following, we consider low symmetry transverse anisotropy for simplicity ($B_4 = 0$). For this model, the diabolical magnetic fields lie in the plane $H_y = 0$ and the other diabolical field components are known analytically [64, 65]:

$$\begin{aligned} H_z &= (M - M')H_z^*, \\ H_x &= (M + M' - 1 - 2n)H_x^*, \end{aligned} \tag{13}$$

where $M, M' = S, S-1, \ldots, -S$ and $n = 0, 1, \ldots, (M + M' - 1)$. The scales $H_z^* = \sqrt{D^2 - B_2^2}$ and $H_x^* = \sqrt{2B_2(D + B_2)}$ are uniquely determined by the anisotropy parameters

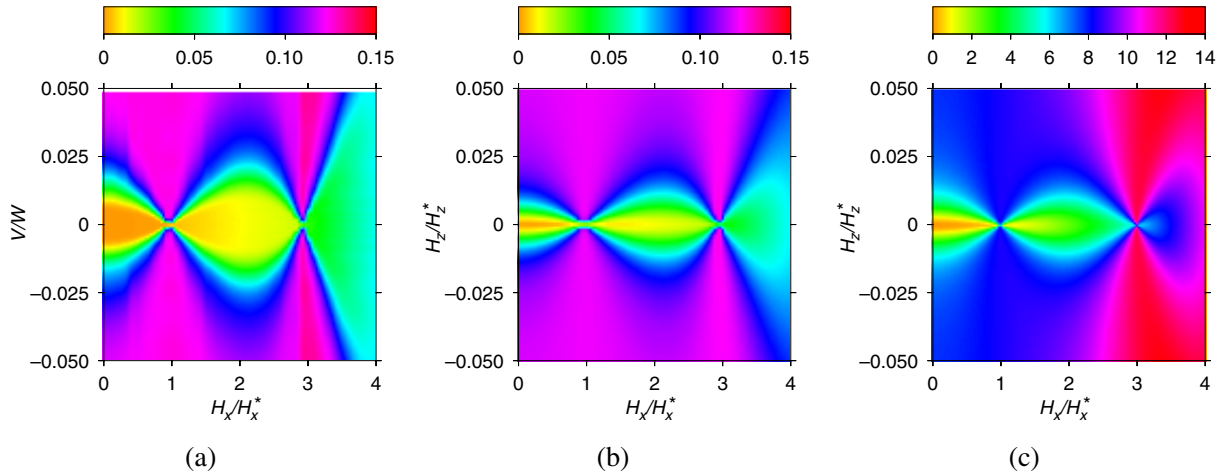

Figure 6. Conductance map as function of the transverse magnetic field H_x and (a) bias V and (b) longitudinal magnetic field H_z. (c) Dependence of the sum of matrix elements $\sum_{i=x,y,z} |\langle g|S_i|g\rangle|^2$ on H_x, H_z. Other parameters: $S = 2$, $J = 0.2$, $D = W = 10B_2$.

D and B_2. We can therefore focus our discussion on the plane $H_y = 0$ and additionally restrict our analysis to $H_x, H_z \geqslant 0$ due to symmetry. In general at a diabolical point multiple pairs of molecular energy surfaces intersect. For the diabolical points with $H_z = 0$ the ground state becomes degenerate, whereas for points with nonzero H_z only excitations cross in energy. We now discuss the effect of the Berry phase associated with interference in the spin reversal. All results were obtained using the NRG, which allows us to access both the weak and strong exchange scattering regime.

5.1. Weak exchange scattering

Since we are mainly interested here in the Berry phase modulation, we will restrict our attention to integer spin S for which the Kondo effect does not develop at $H_z = H_x = 0$ in the weak exchange limit as explained in section 3.1. In figure 6(a), we show the conductance $G(V, H_x)_{H_z=0}$ versus the bias V and the transverse field H_x and in figure 6(b) the zero-bias conductance $G(H_x, H_z)|_{V=0}$ as function of the longitudinal and transverse fields. The two conductance maps in figure 6 show the same striking behaviour: although at zero field H_x one might expect a nearly constant conductance due to the absence of a Kondo peak, we instead find a sharp *dip* at zero bias V or zero field H_z. This central result can be understood by simply considering the cotunnelling transport through the SMM as follows. The pair of states with lowest energy, labelled g, e, are split in energy by an amount δ since the spin-tunnelling B_2 couples spin states with opposite magnetization. For bias V below δ the current involves the ground state g only. In lowest order in J the current is given by the Golden Rule expression for the elastic cotunnelling rate $\propto \sum_{i=x,y,z} |\langle g|S_i|g\rangle|^2$. This rate vanishes because state g (and also e) are characterized by zero expectation value of the spin due to the spin-tunnelling which averages out the magnetic moment. Once the bias window incorporates both states of the pair, nonzero matrix elements $\langle e|S_i|g\rangle$ between the pair of states lead to a nonzero transport current. Along a similar line one can explain the dip as a function of

the field H_z at *zero-bias*: when H_z reaches the initial splitting $\delta_{H_z=0}$ the coherent superposition of states with opposite magnetization starts to be significantly modified, thereby enhancing the current through the ground state g. In figure 6(c) we show the sum of matrix elements $\sum_{i=x,y,z} |\langle g|S_i|g\rangle|^2$, which is responsible for the magnetic field dependence of the Golden Rule cotunnelling rate, as a function of H_x and H_z. It indeed captures the essentials of the NRG result in figure 6(b).

The intrinsic spin-tunnelling on the SMM thus leads to a coherent blockade of transport at low bias and longitudinal field. The width of the suppressed region gives the tunnel splitting δ which can be controlled by the transverse field H_x. This field modulates the Berry phase associated with the spin reversal. At the diabolical points on the H_x-axis the spin-tunnelling between the ground-states is quenched by interference. The lowest two states become degenerate and the dip in the transport closes. In the NRG result a dip of finite width remains exactly at the diabolical point: this is due to higher-order processes in J not incorporated in the Golden Rule argument. The oscillations of the conductance dip correspond to the oscillations observed in time-dependent magnetization measurements which have demonstrated spin-tunnelling effects on SMM crystals [62]. Our results show that transport measurements can directly probe the Berry phase of an *individual* SMM. We point out that no diabolical points with finite $H_z \gtrsim H_z^*$ (related to excited states) can be identified in the limit of weak exchange since the H_x dependence of the conductance becomes featureless. We further note that the question has been raised whether a Kondo effect can occur at the diabolical points [66] with finite transverse magnetic field. In extensive parameters scans we have found no evidence of this, neither in the NRG level flow nor in the spectral function.

5.2. *Strong exchange scattering*

As one increases J towards the strong exchange regime, the small remnant dip in the *bias* dependence of the conductance at the diabolical points on the $H_z = 0$ axis broadens until finally the dip in $G(H_x, V)_{H_z=0}$ is completely independent of H_x (not shown). In contrast to the weak exchange limit, figure 6(a), $G(H_x, V)_{H_z=0}$ is thus not related to the spin-tunnel gap δ due to the strong exchange coupling. However, the H_z-field dependence of the dip in the *zero-bias* conductance $G(H_x, H_z)|_{V=0}$ remains qualitatively the same as in the weak exchange limit (not shown): similar to figure 6(b) the dip follows the tunnel splitting as one varies H_x, allowing all the diabolical points with $H_z = 0$ to be clearly identified.

Qualitatively new is the appearance of the diabolical points at finite longitudinal fields $H_z \gtrsim H_z^*$. This is shown in figures 7(a)–(f) for $S = 1, \ldots, 7/2$. Around the diabolical points the response of the conductance to a change in the magnetic field in the H_x, H_z plane is highly anisotropic. This allows these diabolical points to be identified in an experiment. By counting the diabolical points on the grid (13) and reading off the scales H_z^* and H_x^* one can accurately determine the microscopic parameters S, B_2 and D of the individual SMM. These points involve crossings of excited states only: their appearance in the H_x, H_z dependence of the conductance unambiguously confirms their importance in the strong exchange regime. Finally, we note that the enhancement of the conductance on the $H_x = 0$ axis in figures 7(a)–(f) is due to the Kondo effect. The complicated re-entrant H_z dependence was discussed in [36].

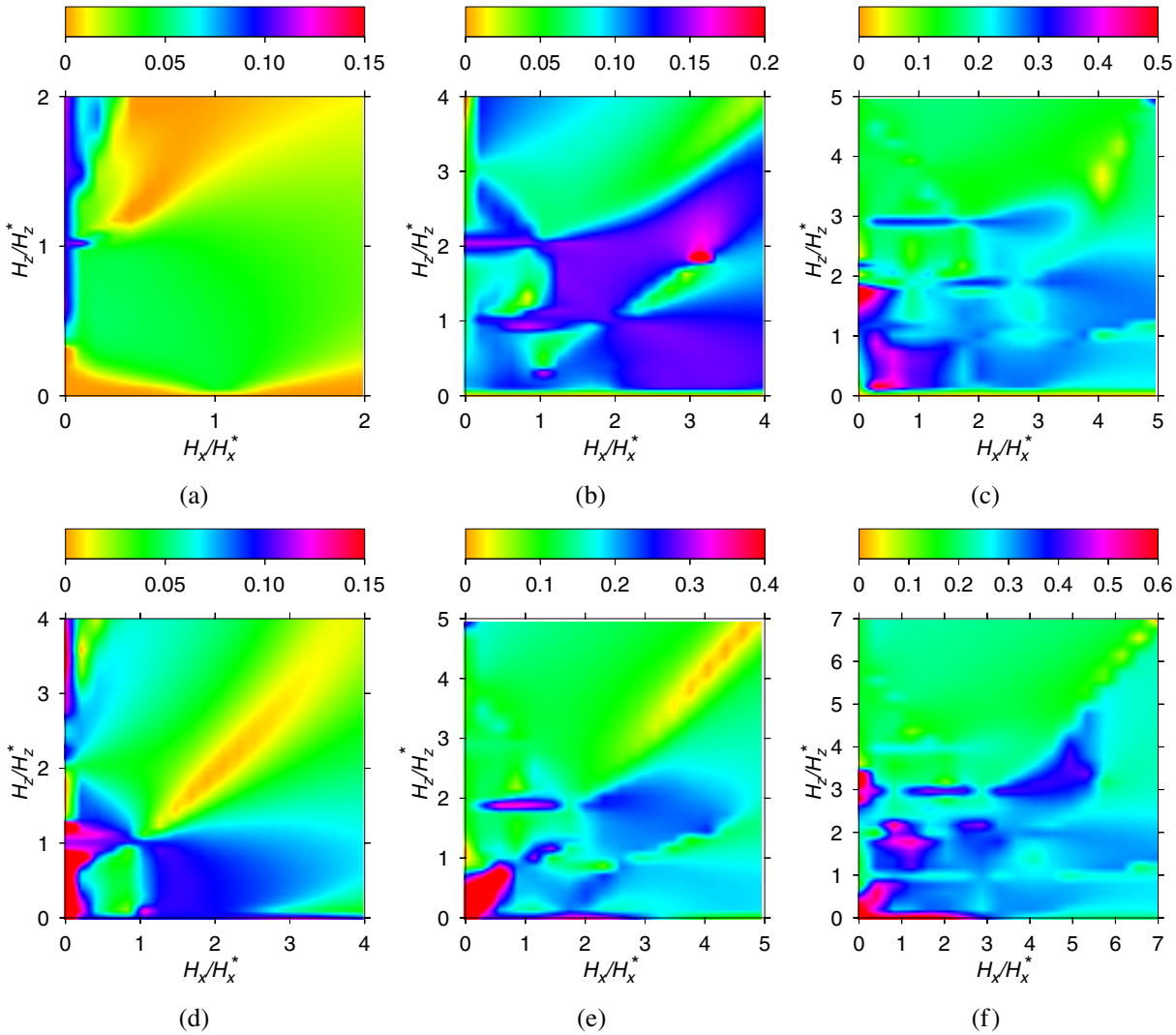

Figure 7. Magneto-conductance map $G(H_x, H_z)_{V=0}$ for subsequent integer spins (a) $S = 1$, (b) $S = 2$, (c) $S = 3$ and half-integer spins (d) $S = 3/2$, (b) $S = 5/2$, (c) $S = 7/2$. Parameters: $J = 0.15$, $D = 10^{-4}$ and $W = 10B$.

6. Conclusion

In summary, we have demonstrated that in the spin-fluctuation regime, the magnetic properties of a SMM embedded in an electric circuit show up clearly in magneto-transport measurements. This includes the strength of the magnetic anisotropy barrier (D), the transverse spin-tunnelling amplitude (B_2, B_4), the orientation of the SMM's anisotropy tensor with respect to the junction electrodes, as well as the *magnetic symmetry* related to the molecular spatial symmetry (B_2 versus B_4). By combining the magneto-transport measurements with the ability to control molecular charge state and the total spin S, and possibly, the molecular geometry through a gate electrode one may gain access to the complete set of microscopic parameters of a SMM transistor.

Acknowledgments

We acknowledge H van der Zant, A Cornia and P Bruno for discussions and financial support of the NanoSci-ERA, the Helmholtz Foundation, the FZ-Jülich (IFMIT) and the EU-RTN for Spintronics.

References

[1] Garg A 1993 *Europhys. Lett.* **22** 205
[2] Heersche H B *et al* 2006 *Phys. Rev. Lett.* **96** 206801
[3] Jo M-H *et al* 2006 *Nano Lett.* **6** 2014
[4] van der Zant H S J *et al* 2006 *Faraday Discuss.* **131** 347
[5] Poot M Osorio E, O'Neill K, Thijssen J M, Vanmaekelbergh D, van Walree C A, Jenneskens L W and van der Zant H S J 2006 *Nano Lett.* **6** 1031
[6] Osorio E A, ONeill K, Wegewijs M R and Stuhr-Hansen N, Bjørnholm T, Paaske J and van der Zant H S J submitted
[7] Park J *et al* 2002 *Nature* **417** 722
[8] Liang W, Shores M P and Bockrath M, J R Long and Park H 2002 *Nature* **417** 725
[9] Pasupathy A N *et al* 2005 *Nano Lett.* **5** 203
[10] Pasupathy A N, Bialczak R C, Martinek J, Grose J E, Donev L A K, McEuen P L and Ralph D C 2004 *Science* **306** 86
[11] Natelson D 2006 *Handbook of Organic Electronics and Photonics* (Valencia, CA: American Scientific Publishers)
[12] Yu L H, Keane Z K, Ciszek J W, Cheng L, Stewart M P, Tour J M and Natelson D 2004 *Phys. Rev. Lett.* **93** 266802
[13] Yu L H and Natelson D 2004 *Nano Lett.* **4** 79
[14] Yu L H and Natelson D 2004 *Nanotechnology* **15** S517
[15] Kouwenhoven L P, Marcus C M, McEuen P L, Tarucha S, Westervelt R M and Wingreen N S, 1997 *Mesoscopic Electron Transport* (Dordrecht: Kluwer) p 105
[16] Kubatkin S, Danilov A, Hjort M, Cornil J, Bredas J, Stuhr-Hansen N, Hedegård P and Bjørnholm T 2003 *Nature* **425** 698
[17] Averin D V and Nazarov Yu V 1990 *Phys. Rev. Lett.* **65** 2446
[18] Ingold G and Nazarov Yu V 1992 *Single Charge Tunneling* (NATO ASI Series vol B 294) (New York: Plenum)
[19] Glazman L I and Raikh M E 1988 *JETP Lett.* **47** 452
[20] Ng T K and Lee P A 1988 *Phys. Rev. Lett.* **61** 1768
[21] Braun M, König J and Martinek J A 2004 *Phys. Rev.* B **70** 195345
[22] Braun M, König J and Martinek J 2005 *Superlatt. Microstruct.* **37** 333
[23] Braun M, König J and Martinek J 2005 *Europhys. Lett.* **72** 294
[24] Wetzels W, Bauer G E W and Grifoni M 2006 *Phys. Rev.* B **74** 224406
[25] Saarikoski H, Wetzels W and Bauer G E W 2007 *Phys. Rev.* B **75** 075313
[26] Martinek J, Barnas J, Maekawa S, Schoeller H and Schön G 2002 *Phys. Rev.* B **66** 014402
[27] Martinek J, Sindel M, Borda L, Barnas J, Konig J, Schon G and von Delft J 2003 *Phys. Rev. Lett.* **91** 247202
[28] Martinek J, Utsumi Y, Imamura H, Barnas J, Maekawa S, Konig J and Schon G 2003 *Phys. Rev. Lett.* **91** 127203
[29] Gatteschi D and Sessoli R 2003 *Angew. Chem. Int. Edn Engl.* **42** 268
[30] Romeike C, Wegewijs M R and Schoeller H 2006 *Phys. Rev. Lett.* **96** 196805
[31] Gonzalez G and Leuenberger M N 2006 *Preprint* cond-mat/0610653
[32] Kim G-H and Kim G-S 2004 *Phys. Rev. Lett.* **92** 137203
[33] Misiorny M and Barnas J 2006 *Preprint* cond-mat/0610556

[34] Misiorny M and Barnas J 2006 *Preprint* cond-mat/0611644
[35] Romeike C, Wegewijs M R, Hofstetter W and Schoeller H 2006 *Phys. Rev. Lett.* **96** 196601
[36] Romeike C, Wegewijs M R, Hofstetter W and Schoeller H 2006 *Phys. Rev. Lett.* **97** 206601
[37] Elste F and Timm C 2006 *Phys. Rev.* B **73** 235305
[38] Timm C 2007 *Preprint* cond-mat/0702220
[39] Lehmann J and Loss D 2007 *Phys. Rev. Lett.* **98** 117203
[40] Cornia A *et al* 2003 *Angew. Chem. Int. Edn Engl.* **42** 1645
[41] Zobbi L *et al* 2005 *Chem. Commun.* 164
[42] Mannini M *et al* 2005 *Nano Lett.* **5** 143
[43] Cornia A, Fabretti Costantino A, Zobbi L, Caneschi A, Gatteschi D, Mannini M and Sessoli R 2007 *Struct. Bond.* at press
[44] Voss S, Fonin M, Rüdiger U, Burgert M, Groth U and Dedkov Yu S 2007 *Phys. Rev.* B **75** 45102
[45] Voss S, Fonin M and Rüdiger U, Burgert M and Groth U 2007 *Appl. Phys. Lett.* **90** 133104
[46] Bencini A and Gatteschi D 1990 *Electron Paramagnetic Resonance of Exchange Coupled Systems* (Berlin: Springer)
[47] Schrieffer J R and Wolff P A 1966 *Phys. Rev.* **149** 491
[48] Wilson K G 1975 *Rev. Mod. Phys.* **47** 773
[49] Hofstetter W 2000 *Phys. Rev. Lett.* **85** 1508
[50] Costi T A 2000 *Phys. Rev. Lett.* **85** 1504
[51] Kikoin K, Kiselev M N and Wegewijs M R 2006 *Phys. Rev. Lett.* **96** 176801
[52] Nazin G V, Qiu X H and Ho W 2003 *Science* **302** 77
[53] Iancu V, Deshpande A and Hla S-W 2006 *Nano Lett.* **6** 820
[54] Temirov R and Tautz F S 2006 *Preprint* cond-mat/0612036
[55] Abrikosov A A 1965 *Physics* **2** 5
[56] Anderson P W 1970 *J. Phys. C: Solid State Phys.* **3** 2436
[57] Hewson A C 1993 *The Kondo Problem to Heavy Fermions* (New York: Cambridge University Press)
[58] Zawadowski A 1980 *Phys. Rev. Lett.* **45** 211
[59] Abramowitz M and Stegun I A 1964 *Handbook of Mathematical Functions with Formulas, Graphs, and Mathematical Tables* (New York: Dover)
[60] Anderson P W, Yuval G and Hamann D R 1970 *Phys. Rev.* B **1** 4464
[61] Tsvelick A M and Wiegmann P B 1983 *Adv. Phys.* **32** 453
[62] Wernsdorfer W and Sessoli R 1999 *Science* **284** 133
[63] Loss D, DiVincenzo D P, Grinstein G 1992 *Phys. Rev. Lett.* **69** 3232
[64] Kececioglu E and Garg A 2001 *Phys. Rev.* B **63** 064422
[65] Bruno P 2006 *Phys. Rev. Lett.* **96** 117208
[66] Leuenberger M N and Mucciolo E R 2006 *Phys. Rev. Lett.* **97** 126601